X-651-73-189
PREPRINT

METEOROLOGICAL INTERPRETATIONS OF THE IMAGES FROM NIMBUS 5 ELECTRICALLY SCANNED MICROWAVE RADIOMETER

T. WILHEIT
J. THEON
W. SHENK
L. ALLISON

JUNE 1973

GSFC
GODDARD SPACE FLIGHT CENTER
GREENBELT, MARYLAND

X-651-73-189

METEOROLOGICAL INTERPRETATIONS OF THE IMAGES FROM NIMBUS 5 ELECTRICALLY SCANNED MICROWAVE RADIOMETER

T. Wilheit

J. Theon

W. Shenk

L. Allison

June 1973

GODDARD SPACE FLIGHT CENTER

Greenbelt, Maryland

METEOROLOGICAL INTERPRETATIONS OF THE IMAGES FROM NIMBUS 5 ELECTRICALLY SCANNED MICROWAVE RADIOMETER

ABSTRACT

The Electrically Scanned Microwave Radiometer (ESMR) on the Nimbus 5 satellite measures microwave radiation in a band centered at 1.55 cm. It scans perpendicular to the satellite motion from 50° to the left to 50° to the right in the 78 steps every 4 seconds producing an image with a best resolution of 25 km.

It is shown that these images can be used to delineate areas of rain over the oceans. This data can be used to approximate the location of fronts, the rain/snow boundary and secondary cyclogenesis.

Page intentionally left blank

CONTENTS

METEOROLOGICAL INTERPRETATIONS OF THE IMAGES FROM NIMBUS 5 ELECTRICALLY SCANNED MICROWAVE RADIOMETER

INTRODUCTION

The Nimbus 5 satellite was launched on 11 December, 1972, into a near-polar orbit (100° retrograde) of about 1100 km altitude. One of the instruments aboard this satellite was the Electrically-Scanning Microwave Radiometer (ESMR) which was the first scanning microwave radiometer to be flown in space. It is the purpose of this article to show that the unique data recorded by this radiometer when displayed pictorially can be meteorologically interpreted over the ocean as showing where areas of rain are occurring which is considerably more difficult with information in the visible and infrared portions of the spectrum.

THE INSTRUMENT

The ESMR receives thermal radiation in a 250 MHz band centered at 19.35 GHz (1.55 m wavelength) with a NEΔT of approximately 2°K. The antenna beam scans from 50° to the left, through nadir, to 50° to the right of the spacecraft track in 78 steps, every four seconds. The half power beamwidth of the antenna is 1.4° at nadir and degrades to 2.2° in the cross track direction at the 50° scan extremes. This corresponds to 25 km resolution at nadir and 45 km in the satellite track direction by 165 km in the cross track direction at the 50° extremes. The instrument and its principles of operation have been discussed by Wilheit (1972).

PHYSICAL PRINCIPLES OF THE ESMR MEASUREMENTS

The physical feature which dominates the data is the tremendous difference in emissivity between the ocean which is typically around 0.4 and that for solid earth surfaces which is usually 0.85 or greater. This results in low brightness temperatures over the ocean (Nordberg et. al., 1970, Hollinger 1971) and high brightness temperatures over land or sea ice (Wilheit et al, 1972, Edgerton et al, 1971, Schmugge et al, 1972).

The cold brightness temperature of the ocean provides a good background for observing the intervening atmosphere. Water vapor and liquid water in the atmosphere both absorb and emit microwave radiation and thus raise the brightness observed over oceans. The exact extent of the effect depends on the temperature and pressure at which the water vapor or liquid water is located but may be roughly expressed for the Nimbus 5 ESMR frequency (Wilheit 1972) by:

$$T_B = A + BV + CL$$

where V is the net water vapor in a column, L is the net non-raining cloud liquid water content, and T_B the resulting brightness temperature.

$$A = 125^\circ K$$

$$B = 6.8^\circ K \text{ cm}^2/\text{gm}$$

$$C = 300^\circ K \text{ cm}^2/\text{gm}$$

Over land, due to the large and highly variable emissivity the effect is ambiguous and thus hard to interpret.

Rain droplets, because of their larger size, comparable to microwave wavelengths, have an enhanced absorption effect (Gunn and East, 1950). This enhancement, combined with the fact that a raining cloud typically contains much more liquid water than a non-raining cloud enables the ESMR to delineate rain areas over the oceans. It is important to note that ice in clouds has no measurable effect in the microwave region so that cirrus clouds or snow offer no effect on the observed brightness temperature. Further discussion of these points along with more extensive references are to be found in Wilheit (1972).

The ESMR data displayed here (Figures 2, 4, 5, 11) are shown in two different dynamic ranges; in each case, the darker image corresponds to roughly 130° to 200°K and the lighter case is 190° to 250°K. For both, dark areas represent the warm end of the dynamic range. In the lower (darker) range we can see gradations in the moisture (liquid and vapor combined) of the atmosphere over the oceans. For a feature to appear even in the lower end of the warmer, darker, dynamic range would require about 10 gm/cm^2 of water vapor or 0.2 gm/cm^2 of liquid water (or an equivalent combination of the two), which is improbable in a non-raining situation. The data away from the near nadir viewing beam positions have been roughly corrected to take out the effects of varying viewing geometry.

CASE I

Figure 1, shows a National Weather Service Radar Summary for 1640 GMT January 22, 1973. Note the band of rain extending from the Middle Atlantic

states, over the Atlantic and across Central Florida into the Gulf of Mexico. The break in the rain shield shown near 30°N, 79° W is an artifact caused by radar station locations and ranges and is almost certainly not a real precipitation echo break. The dotted area shows the region of broken rain and the hatched region indicates the region of solid thunderstorm activity as indicated from the radar return.

Figure 2 shows the ESMR data for the same situation. The relevant portion of the data was taken between 1635 and 1645 GMT of the same day — that is — within five minutes of the radar summary. Such geographic features as the outlines of the Great Lakes, Florida, Cuba and the Isthmus of Panama are easily recognized. The rain area in the Atlantic and Gulf of Mexico shown in the radar summary is obvious in the upper dynamic range. The areal extent of the dark feature indicating rain in the ESMR image is quite close to the areal extent of the broken rain in the radar summary (Figure 1) indicating that the threshold for this dynamic range is comparable to the minimum sensitivity of operational meteorological radar systems (typically 0.2 mm/hr at 50 km range, R. Wexler, priv. comm.). This threshold could vary considerably in these images even though it is set at a constant nominal value of the brightness temperature (190°K) because the constraints of near real-time data processing do not permit calibration of these data to better than about 15°K in the brightness temperature.

A more quantitative study of the relationship between brightness temperature and rain rate is being pursued. This does, however, clearly demonstrate that the ESMR can detect light rain over the oceans.

CASE II

Figure 3, depicts a surface chart for the North Atlantic Coastal area of the United States. Note that snow is indicated all along the coast of New England and Nova Scotia. There are some indications of precipitation from isolated observations over the ocean between the coast and the front which extends northeast and southward from an extratropical cyclone centered at 36°N, 68°W.

In the ESMR image (Figure 4) corresponding to this surface map (2 hours earlier), the rain along the front from as far south as Puerto Rico is clearly visible. It is heaviest just south of Nova Scotia.

Some rain shows along the occluded portion of the front and southeast of the indicated occluded front. There is no indication of rain northwest of this occluded front, but the snow reported at the New England stations would suggest that the precipitation continues in this direction, in the form of snow, to which the ESMR is not sensitive. Thus, we have an indication of a rain/snow boundary in a storm. This boundary is only approximate since snow which melted only a short distance (less than 2 km) above the surface would probably not be detected as rain by the ESMR.

CASE III

In the ESMR image for the Gulf of Mexico area on December 21, 1973, (Figure 5) we see an extensive rain area extending from the northwest corner of the Yucatan Peninsula to North Florida, and a smaller line paralleling the main storm somewhat to the northwest of the main rain band.

Figure 6 is a surface chart for essentially the same time period as the ESMR image. There is rather good agreement with the ESMR data as to the position of the front based on the position of the rain band. There is no information that definitely correlates the position of the main rain band to the front over the ocean; however, it is reasonable to assume that the location of the front is close to this band. This assumption is verified over the adjacent land area north of the Gulf of Mexico.

Figure 7 shows a view of this same area at the same time with the 11.5 μm channel of the Nimbus 5 Temperature Humidity Infrared Radiometer (THIR). This instrument measures radiation in an "atmospheric window" and thus measures cloud top temperature or, if no clouds are present, surface temperature modified by the intervening atmosphere. High clouds appear light (cold) and warm surfaces show up as dark in these images. Most of the Gulf shows up as cloud-covered. There is a cold line along the front indicating the probability of rain but there is no certainty of rain occurrence or of its extent.

The corresponding data from the 6.7 μ m channel of the THIR instrument is shown in Figure 8. This channel is spectrally centered on a strong water vapor absorption maximum. The atmosphere is sufficiently opaque at this wavelength such that clouds and the surface are generally not observed. The colder the signal received, the more water vapor and/or cirrus clouds are present in the upper troposphere. Here one can see a very cold band along the front and a few cool areas northwest of the front. The cold area along the front would suggest rain, however the rain area is more extensive as shown by the ESMR. The cool areas northwest of the front would also suggest some rain. These low temperatures could be caused by thin cirrus with no rain.

The visible portion of the spectrum yields substantially the same sort of information concerning this weather system. The image for this area at 1612 GMT from the visible channel of the Scanning Radiometer (SR) on the NOAA II satellite has been examined. The relevant details of the image would not survive publication printing so it is not included. As in the infrared images, there were dense clouds along the front and rather solid clouds to the northeast of the front, but it was not possible from this image alone to determine the extent or even the existence of rain associated with this front.

The radar summary shown in Figure 9 shows some of the rain over the water but misses most of it due to range problems. Thus, the microwave image provides important meteorological information concerning rainfall available from

neither conventional surface observations, simply because of inadequate station locations, nor from visible or infrared satellite observations.

CASE IV

The last example shows how the ESMR measurements can be used to improve the analysis of conventional meteorological charts and for the detection of the early stages of cyclogenesis associated with secondary cyclones. Figure 10 shows the surface chart for the North Pacific region for 0000 GMT, December 13, 1972 and Figure 11 is the ESMR image for the same area some 13 hours later. The frontal system shown in the surface chart is seen in the lower brightness range of the ESMR image but only a small linear feature appears in the upper brightness range (34° N, 158° E to 40° N, 162° E) indicating that there is little if any rain throughout this frontal system and the increased microwave brightness temperature is probably due to the increase of cloudiness associated with the fronts. Most likely this feature is associated with a warm front extending southeastward from a triple point at 45°N, 162°E, an occlusion extending to the northwest, and a cold front to the south and southeast. Along this warm front a secondary cyclone is starting to form (36°N, 170° E) and is shown in the surface analysis. At this point there is an indication of rain in the upper brightness range ESMR image, which confirms the early stage of cyclogenesis. Shenk (1970) discovered that a strong rise of cloud top heights, as determined from infrared cloud top temperature measurements, southeast of a primary cyclone center was an indication that secondary cyclone cyclogenesis was imminent. The development of increased rainfall intensity should serve as a similar indication.

CONCLUSIONS

We have shown that the ESMR data add a new dimension to the remote sensing of meteorological data from satellites. The ESMR is capable of detecting and mapping rainfall areas over oceans (case I), and identifying the rain-snow line in winter precipitation (case II). This information cannot be reliably obtained from remote sensors utilizing visible and infrared spectra (case III) and further, the detection of rainfall can be used to predict secondary cyclogenesis (case IV). This instrument should prove to be a powerful tool in weather observation, forecasting and research by providing information that was heretofore been unavailable on a global scale: The distribution and, hopefully, the intensity of rainfall over oceans.

ACKNOWLEDGEMENT

The authors wish to acknowledge the contribution of Dr. Patrick Thaddeus of the Goddard Institute for Space Studies, who originated the experiment concept and who served as principal investigator in the formative stages of its development.

REFERENCES

Edgerton, A. T., F. Ruskey, D. Williams, A. Stogryn, G. Poe, D. Meeks and O. Russell, "Microwave Emission Characteristics of Natural Materials and the Environment", Microwave Division, Aerojet General Corp., ONR Contract NOOD 14-70C-0351, 1971.

Gunn, K. L. S. and T. U. R. East, "The Microwave Properties of Precipitation Particles", Quart. J. Met Soc., 80, 522-545, 1954.

Hollinger, J. P., "Passive Microwave Measurements of Sea Surface Roughness", Trans. IEEE Geoscience Electronics, GE-9, pp 165-169 (1971).

Nordberg, W., J. Conaway, D. B. Ross, and T. Wilheit, "Measurements of Microwave Emission from a Foam-Covered Wind Driven Sea", J. Atmos. Sci., 28, 429-435, 1971.

Schmugge, T., P. Gloersen, and T. Wilheit, "Remote Sensing of Soil Moisture with Microwaves", NASA X-652-72-305 (Aug. 1972).

Shenk, W. E., "Meteorological Satellite Infrared Views of Cloud Growth Associated with the Development of Secondary Cyclones", Monthly Weather Review 98, 861-868, 1970.

Wilheit, T. T., "The Electrically Scanning Microwave Radiometer (ESMR) Experiment", in the Nimbus 5 User's Guide, Ed. by Romeo R. Sabatini. ERTS/Nimbus Project, Goddard Space Flight Center, National Aeronautics and Space Administration (Nov. 1972).

Wilheit, T., W. Nordberg, J. Blinn, W. Campbell, and A. Edgerton, "Aircraft Measurements of Microwave Emission from Arctic Sea Ice", Remote Sensing of Environment, 2, 129-139 (1972).

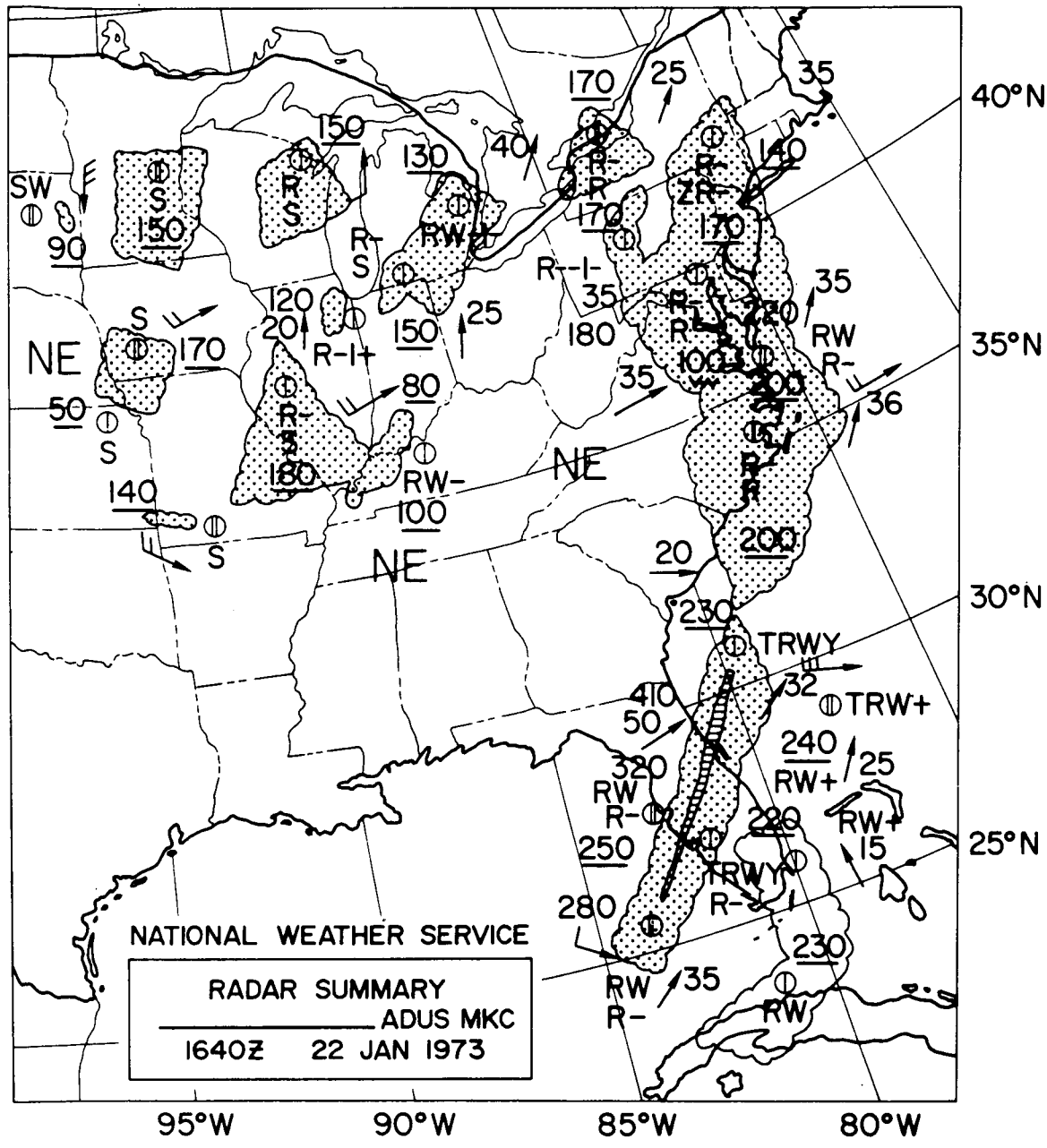

Figure 1. A radar summary corresponding to the ESMR image in Figure 2. The break in the radar return is an artifact caused by station locations and does not coincide with the similar artifact in the ESMR image.

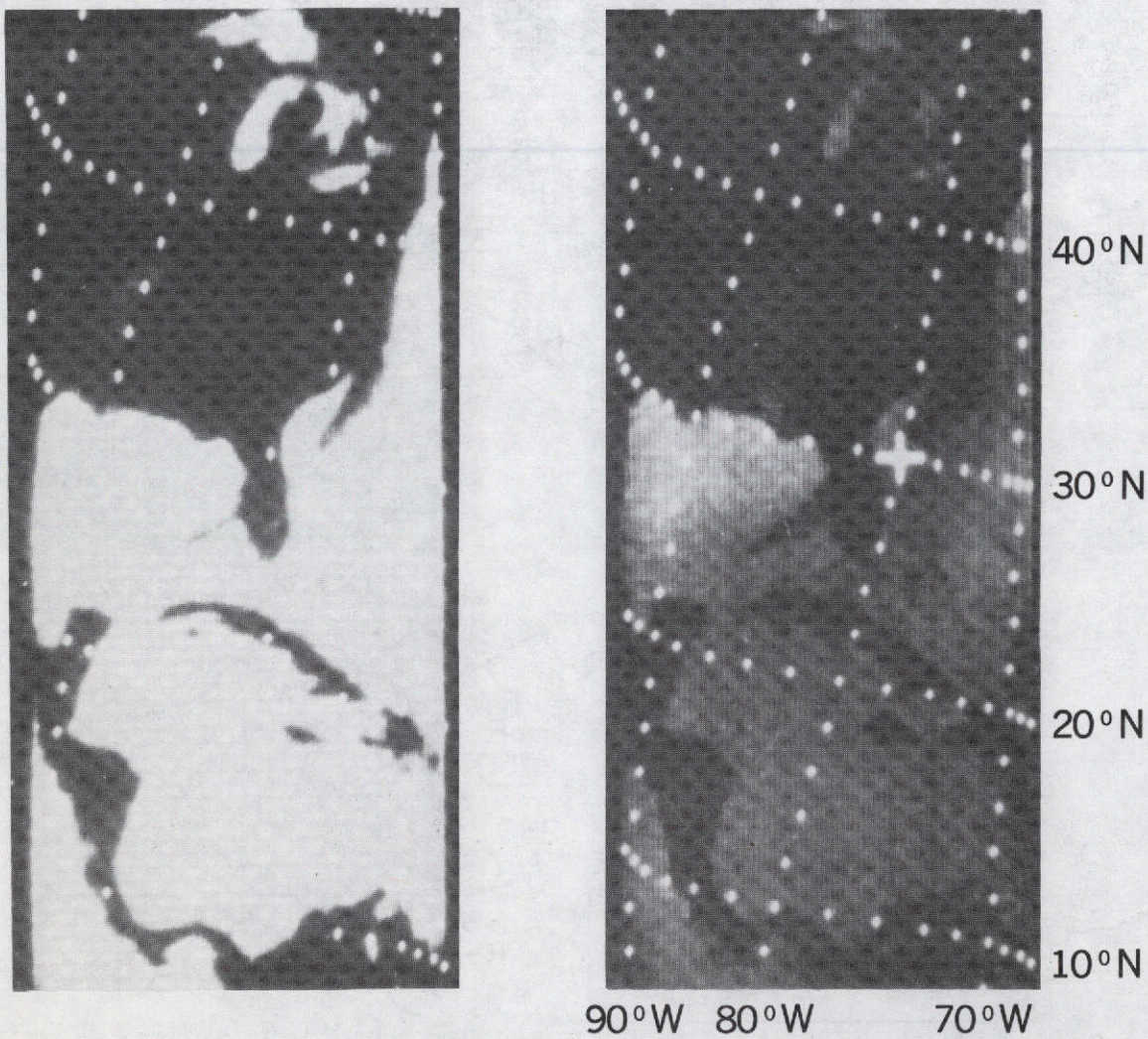

Figure 2. An ESMR image showing a front with rain activity extending from the North Carolina coast into the Atlantic, across Florida and into the Gulf of Mexico. The image on the left has a dynamic range of from 190°K to 250°K and that on the right from 130°K to 200°K. The apparent break in the rain is an artifact caused by the Fiducial Mark at 30°N, 80°W.

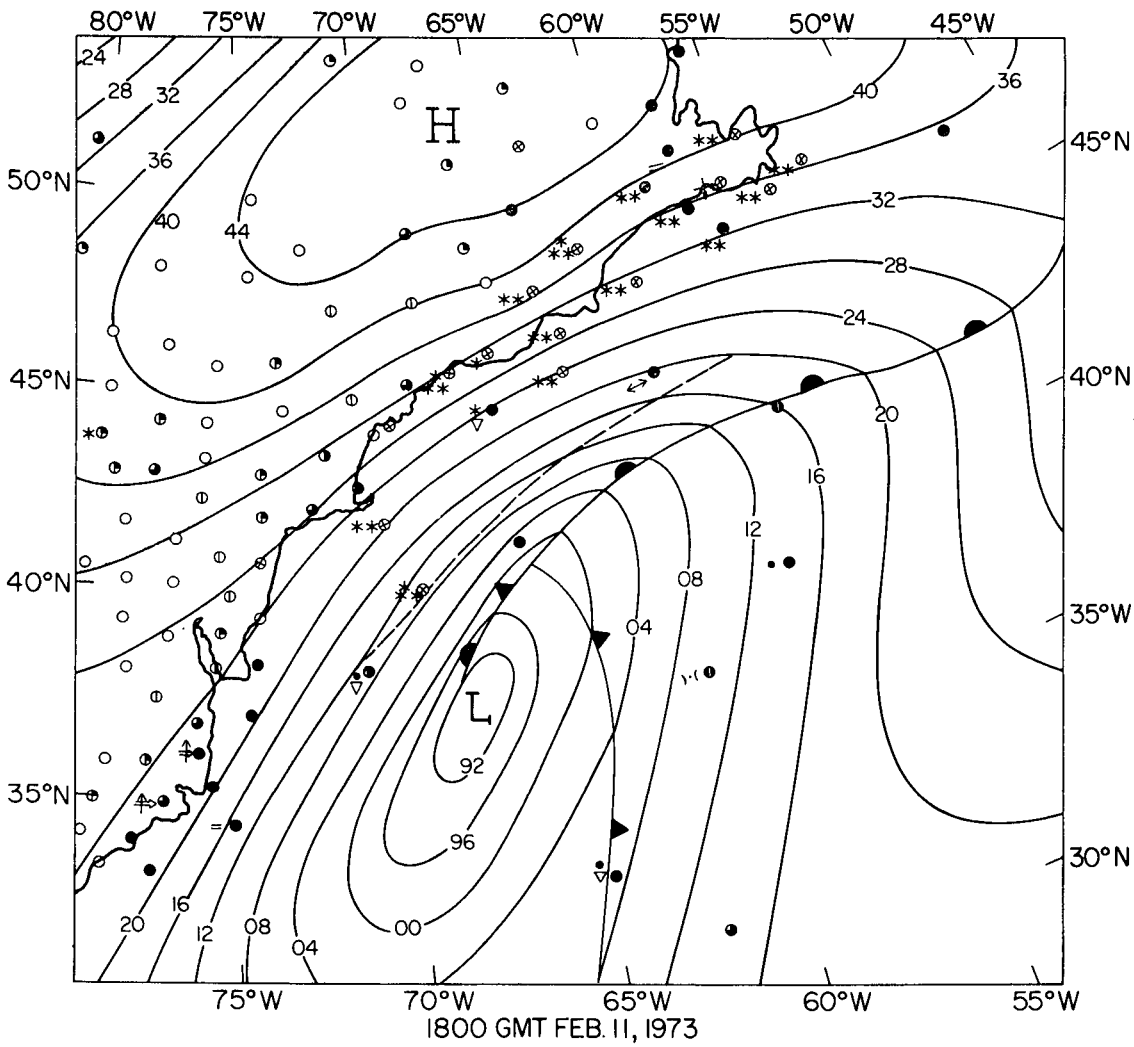

Figure 3. Surface chart for 1800 GMT Feb. 11, 1973. The sky condition and present weather symbols, one shown for each station and the estimated boundary between snow and rain at the surface over the ocean is indicated by the dashed line northwest of the warm and occluded fronts.

NIMBUS 5 ESMR
JANUARY 11, 1973
1541-1557 GMT

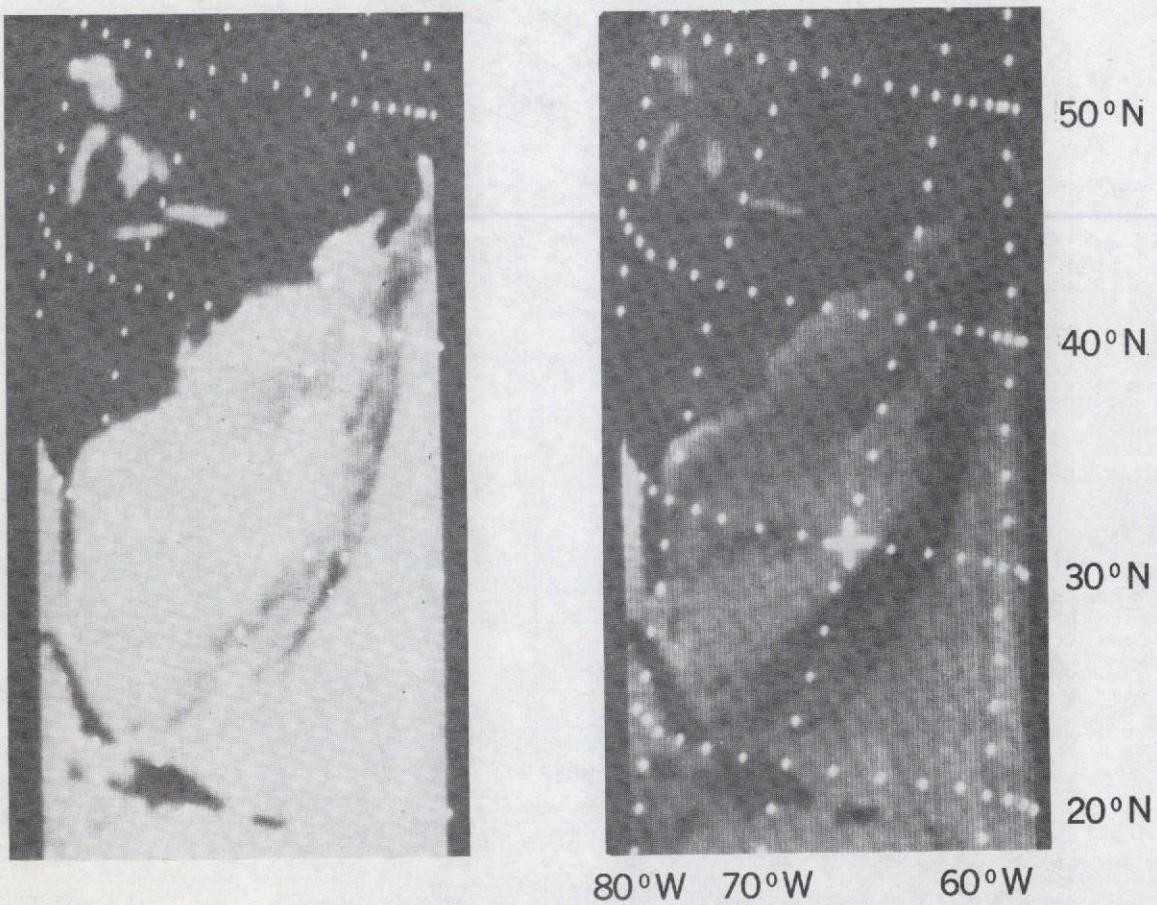

Figure 4. The ESMR image corresponding to the surface chart in Figure 3. The 190°K to 250°K range is shown on the left and the 130°K to 200°K range is on the right.

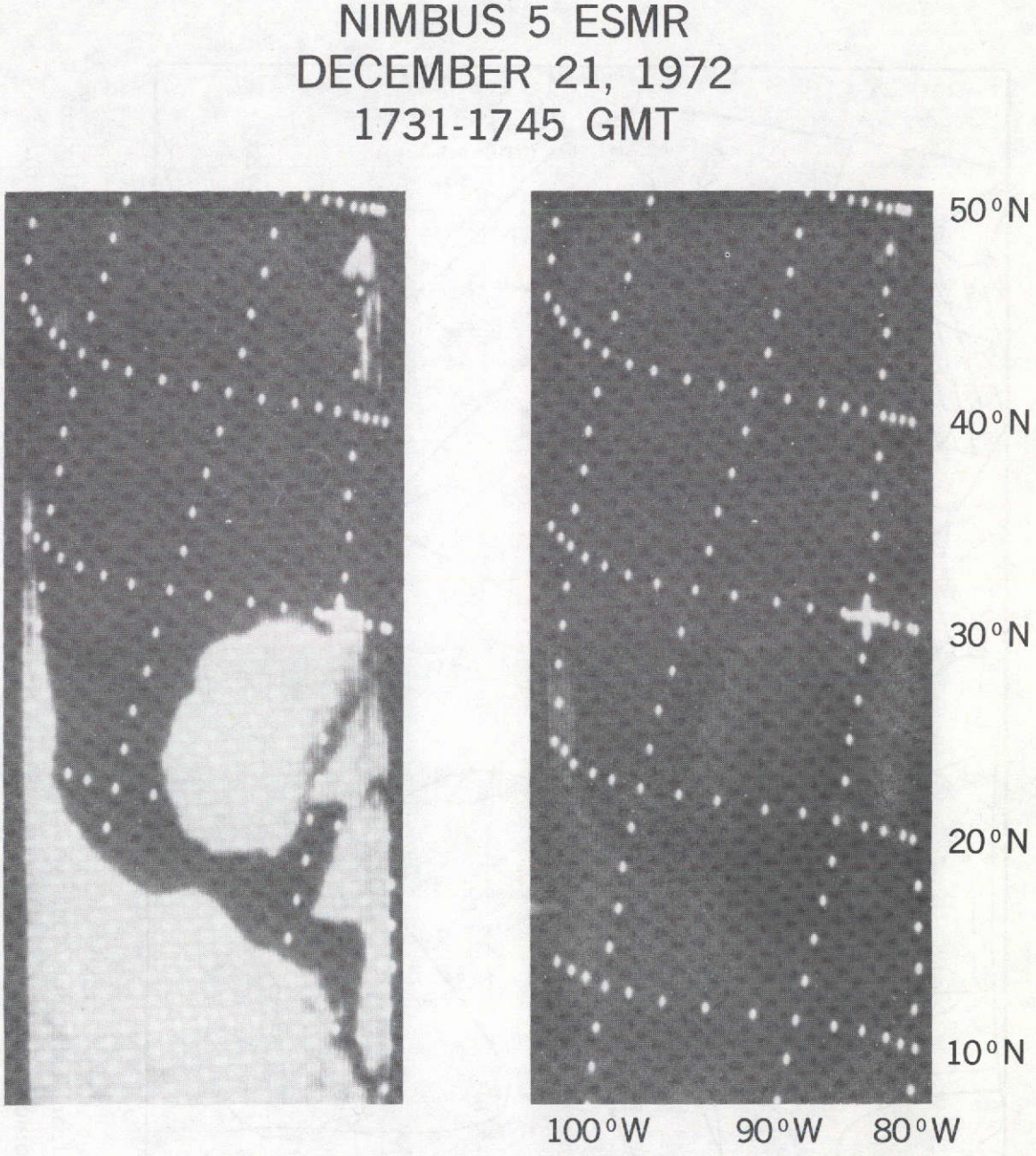

Figure 5. An ESMR image showing a band of rain extending from North Florida across the Gulf of Mexico to Yucatan. The 190°K to 250°K range is on the left and the 130°K to 200°K range is on the right.

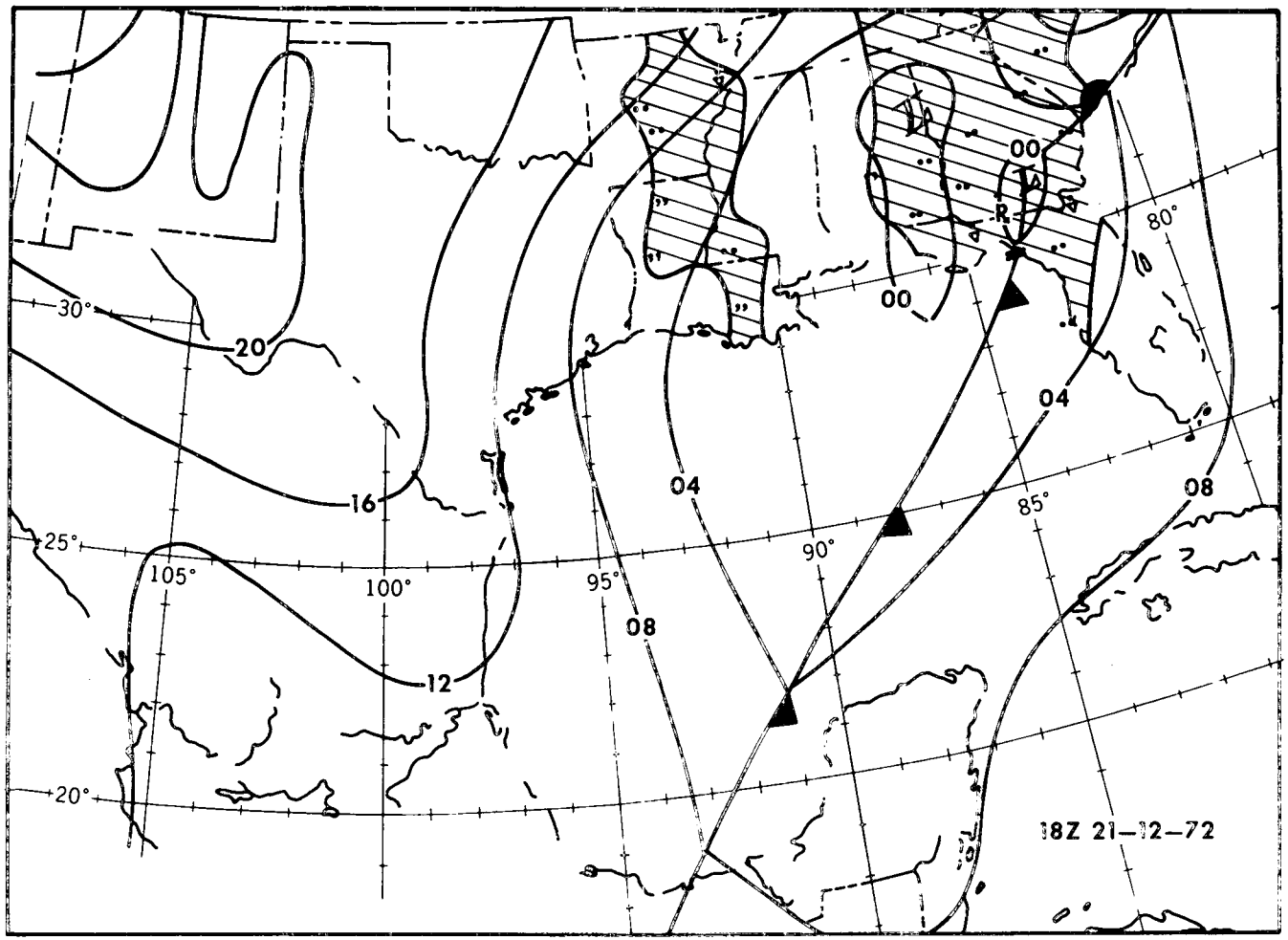

Figure 6. Surface chart for 1800 GMT Dec. 21, 1972.
The front extending southwestward from southeast Georgia across the Gulf of Mexico coincides quite closely with the rain band observed in the ESMR image (Fig. 5).

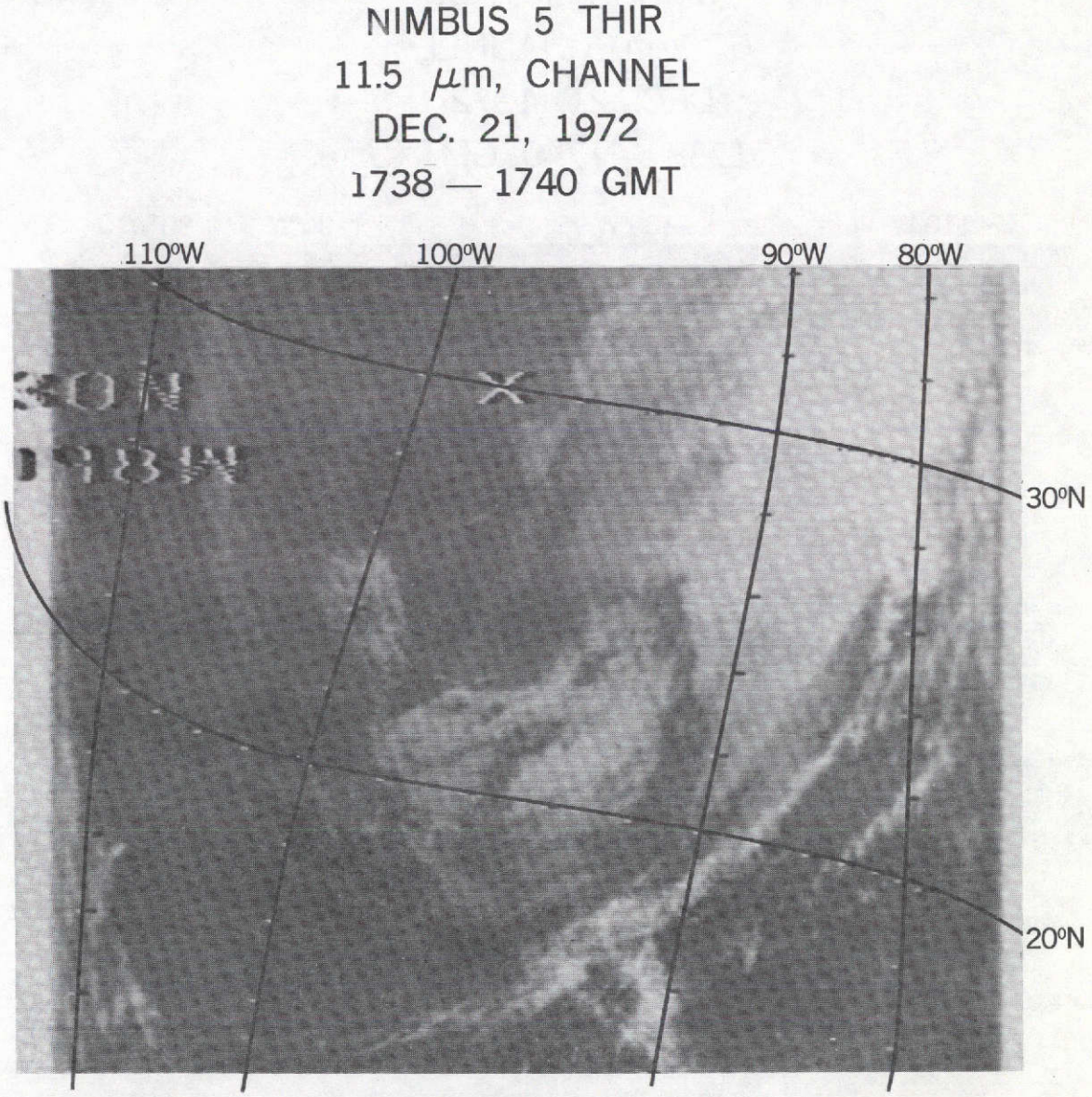

Figure 7. An infrared window (10.6μm) image from Nimbus 5 THIR corresponding to the ESMR image (Fig. 5) cold (high) clouds appear as light tones.

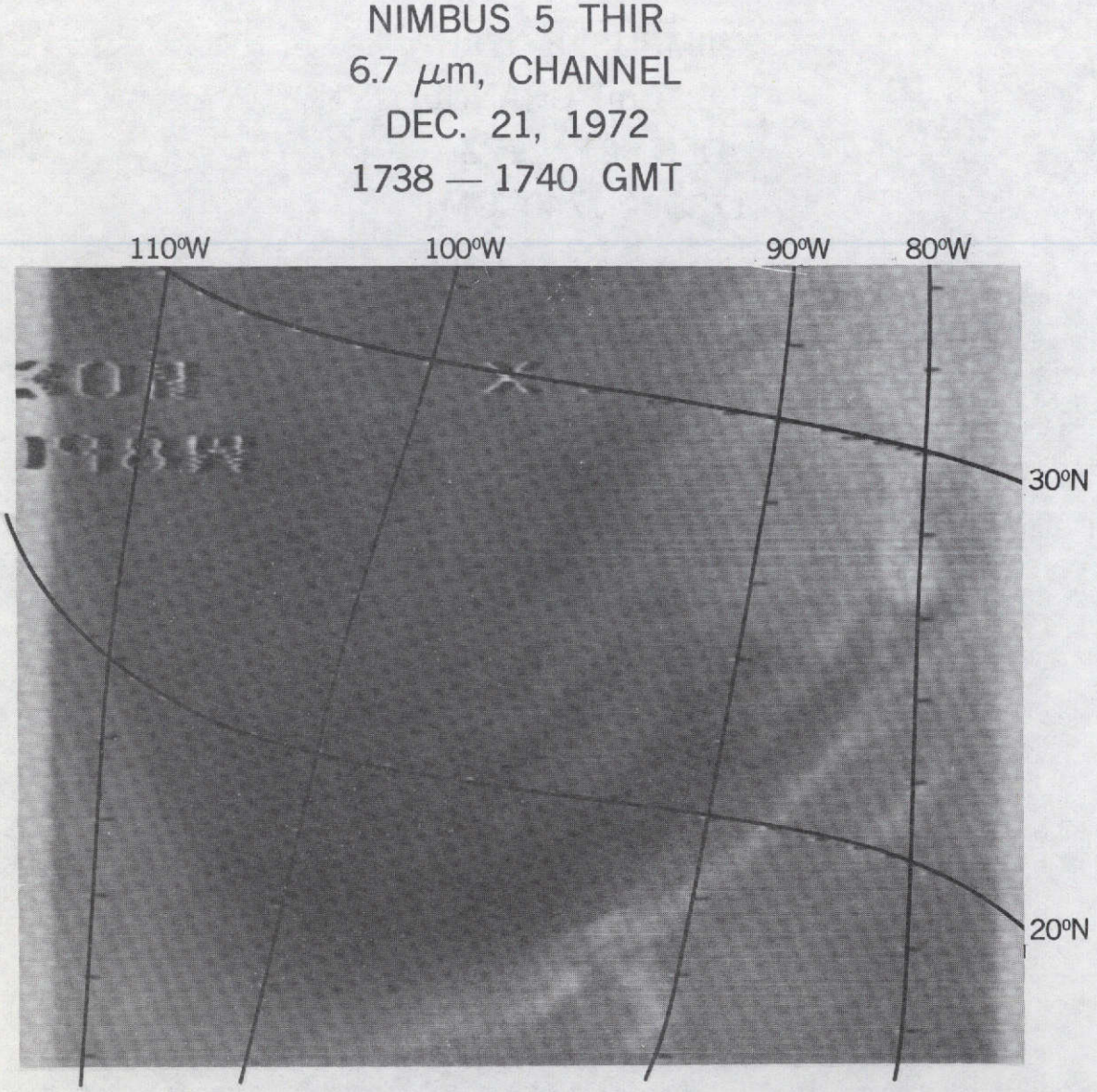

Figure 8. An infrared water vapor (6.7 μm) image from Nimbus 5 THIR corresponding to the ESMR image (Fig. 5). Light tones indicate water vapor and/or cirrus clouds in the upper troposphere.

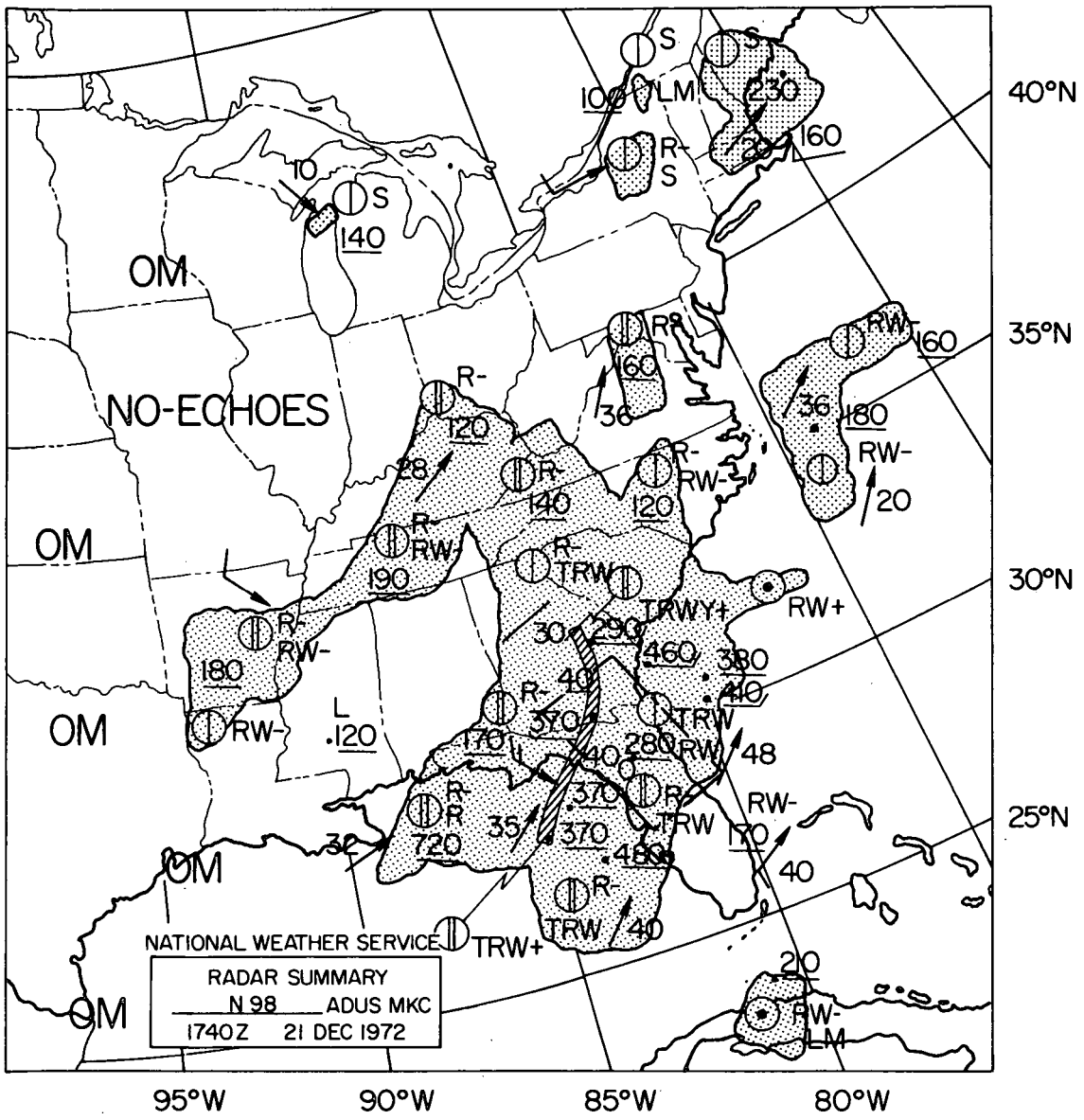

Figure 9. Radar summary corresponding to ESMR image (Fig. 5). Due to range problems the data does not extend very far into the Gulf of Mexico.

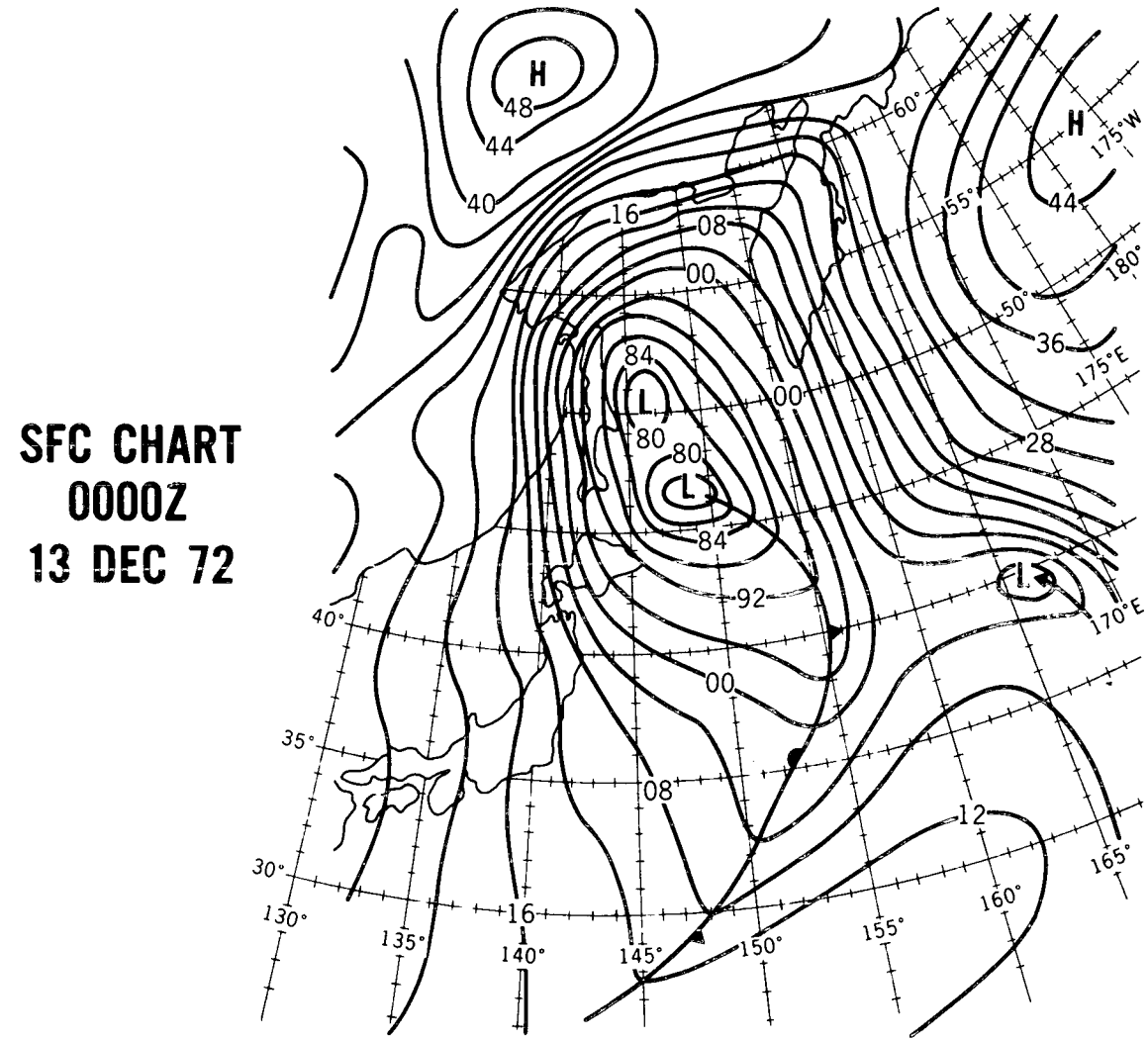

Figure 10. Surface chart showing frontal system in the North Pacific.

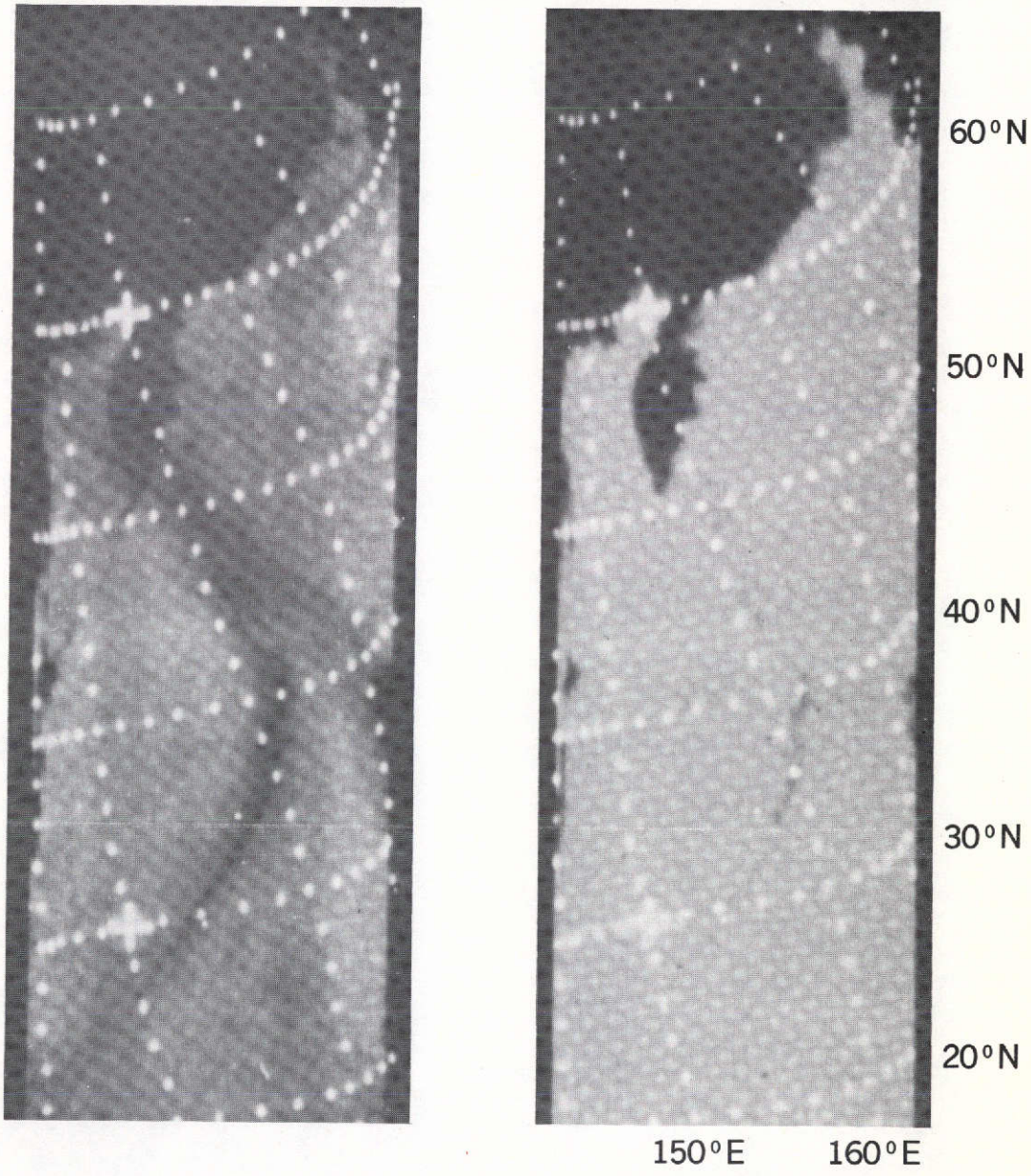

Figure 11. ESMR image showing frontal system in North Pacific. The details differ grossly from the corresponding surface chart (Fig. 10). The 130°K to 200°K range is on the left and the 190°K to 250°K range is on the right.

☆ U.S. GOVERNMENT PRINTING OFFICE: 1973—734-722/47